Polymer 95 (2016) 45–51

Contents lists available at ScienceDirect

Polymer

journal homepage: www.elsevier.com/locate/polymer

Vitrification and plastic flow in transient elastomer networks

Robyn H. Pritchard [a], Anna-Lena Redmann [a], Zhiqiang Pei [b], Yan Ji [b], Eugene M. Terentjev [a, *]

[a] Cavendish Laboratory, University of Cambridge, Cambridge CB3 0HE, UK
[b] Department of Chemistry, Tsinghua University, Beijing 100084, China

ARTICLE INFO

Article history:
Received 5 February 2016
Received in revised form
23 March 2016
Accepted 25 April 2016
Available online 26 April 2016

Keywords:
Vitrimers
Rubber elasticity
Transient network
Liquid crystal elastomers

ABSTRACT

We investigate how the crossover temperature of the elastic-plastic transition, the 'vitrification point' T_v, changes under load for isotropic vitrimers and exchangeable liquid crystal elastomers (xLCEs), using the thermoplastic SIS triblock polymer as a reference. In all these cases, the elastic network cross-links are transient: physical micro-phase separation in SIS and covalent transesterification bonds in vitrimers. From the analysis of SIS we define T_v as the point when entropic rubber-elasticity contraction due to heating under load turns into the irreversible plastic extension due to cross-links breaking and reforming. In xLCEs, the response to mechanical stress is heavily influenced by the smectic liquid-crystalline order, which makes the material much stiffer than normal rubbery networks, and also leads to the shape-memory effect across the smectic-isotropic transition point. The vitrification in the isotropic phase of xLCE, and in isotropic vitrimers, was found to be independent of stress, which can be attributed to the thermal activity of the catalyst determining T_v and it not being mechanically coupled to the elastic network. Beyond T_v, with increasing stress the plastic extension rapidly increases with temperature, as cross-link dynamics becomes more apparent.

1. Introduction

Cross-linked polymers are essential in many applications and the understanding of their mechanical properties leads the way to improved materials and new technological developments. When the cross-linking is relatively weak, that is, long strands of polymer chains are connecting the junction points, the material behaves as an elastomer above its glass transition. Depending on the nature of the cross-links (permanent covalent bonds or non-permanent physical bonds), the resulting polymer networks are classified as thermoset or thermoplastic elastomers, respectively. Permanent bonds give excellent mechanical strength, thermal stability and solvent/environmental resistance – however, once the cross-linking reactions are finished, the elastomer cannot be reprocessed or reshaped. In contrast, the cross-linking of thermoplastic elastomers usually occurs by a thermally-activated process, such as local crystallization, glass transition, or just microphase separation. The ability of such transient networks to plastically flow when heated makes it possible to reshape, repair and recycle them. These are desirable properties that sometimes offer an advantage over chemically cross-linked elastomers; however, the lack the durability of thermosets limits their use.

The idea of transient networks, in which cross-linked sites undergo continuous rupture and reformation, thereby relaxing local stress in strained systems, has been known for some time [1,2]. Examples of physical (non-covalent) bonds that can lead to transient behavior include hydrogen bonding, charge (electron) transfer, ion pairing, acid-base interaction, dipole-aromatic ring interaction, and coordination with metallic ions. In water-based gels, the hydrophobic interaction could also be a cause of transient network formation. The binding forces range from strong ionic interactions to weak dispersive interactions. On the larger scale of multi-block copolymers, a common example is styrene-isoprene-styrene (SIS) triblock copolymer, in which the transient elastomer network is of 'telechelic' morphology where phase-separated minority end-blocks [3,4] form a glass while the middle blocks remain in the thermally mobile elastomeric state. We use SIS in this work as a reference transient network (see Fig. 1).

A new class of polymeric materials, known as vitrimers, bridges the gap between thermoset and thermoplastic elastomers. Vitrimers are thermally moldable elastomers with covalent bonds made reversible by transesterification exchange reactions, which results

* Corresponding author.
E-mail address: emt1000@cam.ac.uk (E.M. Terentjev).

http://dx.doi.org/10.1016/j.polymer.2016.04.060

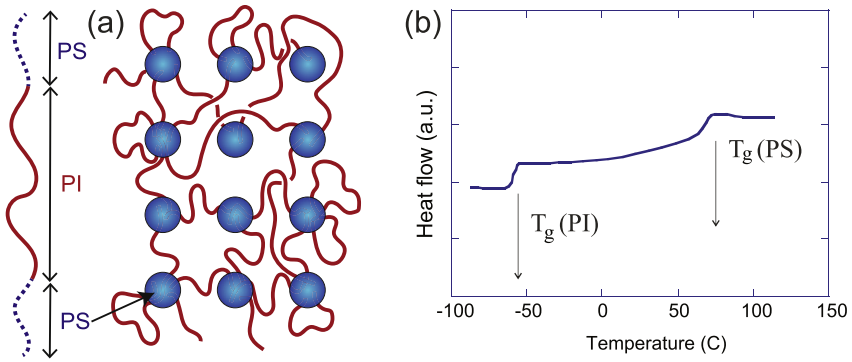

Fig. 1. (a) A scheme of SIS triblock structure and the morphology of micro-phase separated elastomer network with PS micelles in the glassy state. (b) The DSC scan of 14 wt% SIS showing the glass transitions of PI and PS blocks, respectively, with T_g(PS) ≈ 75° [20]. The vitrification temperature T_v, determined later in the paper, is also marked in order to illustrate the lack of any thermal signature in its region.

in the combination of the processability of thermoplastic elastomers with the mechanical robustness of thermoset elastomers [5,6]. In fact, transesterification is not the only possibility for such exchangeable covalent bonds [7]. The transesterification (hydroxy − ester exchange) has a reaction rate depending on temperature in an Arrhenius activation manner; it allows a rearrangement of the network topology while keeping the total number of covalent cross-links constant in a much more robust way than other transient processes, see Fig. 2. The transesterification reactions can only take place when a catalyst is included in the vitrimer [8] and the catalyst concentration can be used to control the transition temperature [9]. Even in the presence of a suitable catalyst, due to a very slow reaction rate at low temperatures, the network topology is frozen, while above a characteristic temperature the fast transesterification exchange enable a relaxation of externally applied stress via a plastic deformation of the network. Leibler et al. have called this temperature the 'vitrification transition', T_v. Much of this paper is dedicated to the analysis of this transition in different materials and methods of analysis, and contrasting it with the transition to the plastic-flow regime in a physically cross-linked telechelic SIS elastomer.

Networks with exchangeable covalent bonds have a great potential as liquid crystal elastomers. Liquid crystal elastomers (LCE) are active polymers capable of converting external stimuli into mechanical actuation [10]. Even though this is a very useful property for many applications, it could not be easily utilized because a uniform macroscopic liquid crystalline order is hard to achieve in practice. It has been recently shown that this limitation can be overcome by introducing exchangeable covalent bonds as cross-links, resulting in the abbreviation xLCE for these new 'exchangeable' liquid crystal elastomers [11]. Like in the case of ordinary isotropic vitrimers, a catalyst must be added to the polymer network to allow for transesterification reactions to take place. xLCEs undergo three transitions upon heating: in addition to a glass transition at low temperatures and a vitrification transition at high temperatures, which are both seen in other vitrimers as well, xLCE also has a liquid-crystal to isotropic transition at an intermediate temperature T_i [11]. In the materials we are studying in the paper, the liquid-crystalline phase is smectic A, which causes the mechanical rigidity of the sample in this state to be quite high [12,13]. The locking of network cross-links by smectic layers does allow smectic elastomers to function as a multiple shape-memory material [11,14–16]. However, in order to establish xLCEs as a technologically useful material, their mechanical properties and the transitions they undergo have to be understood in greater detail.

In this work, we study the transition from a fully elastic to a plastic-flow regime on increasing the temperature under constant tension. We carried out elongational creep experiments on polydomain xLCE samples with and without catalyst, and compared that with SIS as a reference thermoplastic system, and also with the ordinary non-LC vitrimers of Leibler et al. We applied different values of constant tensile stress σ_0 in order to assess how (or whether) the characteristic transition temperatures vary under an external mechanical field. The elongation of the sample as a function of temperature $\varepsilon(T)$ was measured, which directly gives the creep compliance under constant stress via $\varepsilon(T) = J(T)\cdot\sigma_0$; in the elastic regime the creep compliance is the inverse of the Young modulus, while in the plastic-flow regime it reflects the rate of strain response.

2. Experimental methods

2.1. Materials

The SIS symmetric triblock copolymer with 14 wt% fraction of

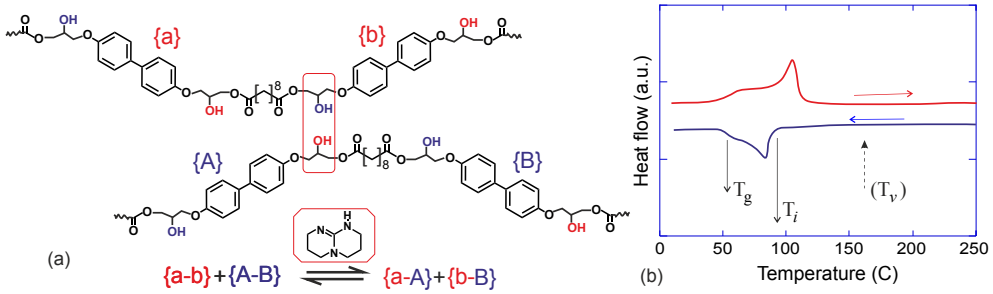

Fig. 2. (a) The chemical structure of xLCE chains, with mesogenic groups alternating with flexible C_8 spacers, and the scheme of reversible transesterification in the presence of TBD catalyst. (b) The DSC scan of xLCE showing the glass transition and the smectic-isotropic transition, T_g and T_i points, respectively. The vitrification point does not appear to have a thermal signature; a point T_v is also marked from our creep-experiment analysis below.

polystyrene (PS) end-blocks was obtained from Sigma–Aldrich. We performed gel permeation chromatography (GPC) to verify the molecular weight and polydispersity, which was less than 1.1, while the overall molecular weight of the middle polyisoprene (PI) block was ca. 210,700. The glass transitions of each component are widely separated. The bulk polyisoprene (PI) has a very low $T_g \approx -70$ °C [17]; the bulk atactic polystyrene has $T_g \approx 100$ °C [18]. In small volumes of micro-phase separated PS micelles of block-copolymer, the upper glass transition T_g(PS) is suppressed, while the glass transition of PI is elevated. Fig. 1 (b) shows the two glass transitions in the SIS used in this work. Previous studies have shown that at temperatures well below T_g(PS) the solid micelles provide a sufficient anchoring for the polyisoprene chains and the material is fully elastomeric, while at higher temperatures the energy barrier for pullout of a polystyrene tail from a softening micelle becomes lower and the network can flow plastically under stress [4,19]. Here we aim to study how this transition can be accurately detected, and how it changes depending on the magnitude of the applied stress (or the level of elastic energy density in the network).

The SIS samples were prepared by pressure molding. The SIS pellets were poured into a rectangular hole in a metal plate of 5 mm thickness, which was then covered by a PTFE sheet and a rigid aluminum plate on each side. This was pressure molded at 135 °C, which is well above the T_g, under a pressure of 300 lbf/in^2 [2.1 MPa] for 60 min, after which it was allowed to cool at room temperature. In a next step, the sample was pressure molded again but this time for 30 min between two pieces of folded aluminum foil, which was used as spacer to mold the SIS rectangle to a thickness of approximately 0.25 mm. This procedure leads to a flat, homogeneous and optically transparent elastomer sheet, where the original particle structure is no longer visible. After letting the SIS sheet cool to room temperature, rectangular sample strips of ~0.25 mm thickness, ~5 mm width, and ~20 mm length were cut. The sample width and thickness were measured at several positions using verniers and the average value of the sample cross-section area was used for stress calculation.

The xLCE samples were synthesized in the lab following a procedure described previously [11], see Fig. 2(a). After the final step of the reaction, a 1:1 mixture of 4, 4-dihydroxybiphenyl mesogen and sebacic acid spacer was cured by pressure molding the polymer mixture at 180 °C under a pressure of 300 lbf/in^2 [2.1 MPa] to form a cross-linked network. Two variants were prepared: one with the triazabicyclodecene (TBD) catalyst added at 5 mol%, and the other without the catalyst (to investigate its role on the vitrification process under stress). With the catalyst present, the bonding of the network at such a high temperature was quick and the pressure molding for 30 min was sufficient. In the case of no catalyst, this reaction took a very long time and the pressure molding was carried out for over 6 h to achieve a good network. To verify the completeness of network cross-linking and the full conversion of the epoxy groups of each monomer, in each case we subjected each sample to swelling in a large amount of 1:1 mixture of methanol and DCM to reach a 10-times volume increase over 30 min. It was verified that during this 'washing' procedure the catalyst was retained inside the network: it is not obvious that this should be the case (and we explain it by hydrogen bonds forming between the NH-group of the catalyst and several complementary moieties on the polymer chain, see Fig. 2) – but we have found no difference in either thermal transitions or the creep experiment for the catalyst-containing samples before or after this swelling procedure, in great contrast with the samples that originally contained no catalyst (see Fig. 8 below).

To investigate the role of transesterification in the vitrification transition, we also prepared two other materials containing exactly the same hydroxy-ester chemical groups but slightly different monomer groups. In the original xLCE we used the rod-like mesogenic biphenyl moiety, which orders into smectic layers below T_i. In the xLCE2 material, we used the same biphenyl group but with a longer and more flexible spacer (Fig. 3), which leads to a much lower temperature of liquid-crystalline transition.

Finally, we also prepared the classical isotropic vitrimer network of Leibler et al. [5] where the monomers are non-mesogenic, so that there is no liquid crystalline phase, and only the glass transition point is evident in the calorimetry scan, Fig. 4. In all cases, the molar fraction of hydroxy and ester groups, and the TBD catalyst content, were kept exactly the same to make meaningful comparisons of thermo-mechanical behavior. After curing, rectangular sample strips of ~0.2 mm thickness, ~5 mm width, and ~20 mm length were cut from each elastomer for tensile testing.

2.2. Creep experiment

The main experimental method we use is sometimes incorrectly called 'dilatometry'. The term dilatation refers to the change of volume, whereas the solvent-free elastomer (or plastically flowing polymer melt) will keep their volume constant above the glass transition. We carry out the classical creep compliance experiment, which is an inverse of stress relaxation and probes the change in strain (extension ratio) with time at a constant tensile stress applied to the sample – at constant temperature to test relaxation or at increasing temperature to probe the changes in cross-linking nature of the network. In particular, we look for the onset of 'creep', or plastic flow, under tensile stress as the temperature increases above T_v and the material gradually changes its phase from a strictly elastic network to a plastically deformable transient network, and eventually to a polymer melt.

Our creep measurements were carried out in a custom-built thermo-mechanical device. Since test temperatures as high as 300 °C were required, while continually monitoring the sample length inside and maintaining the constant tension at all times, the technical demands on such thermal chamber were high. It consisted of an electrically heated aluminum box, insulated from the outside with glass wool filling the space between the walls of the outside box made of PTFE. The temperature in the chamber could be increased from ambient to 300 °C at a constant rate of ca. 5°/min, and monitored with thermocouples at several positions inside the box (to assure the homogeneous temperature distribution). Constant stress was maintained with the bottom clamp attached to the base of the chamber and the top clamp attached to a load cell mounted on computer controlled motorised stage. The stage and loadcell were thermally isolated outside the box and coupled to the top clamp through a rod that entered the heating chamber, to minimize temperature change altering the load cell reading. The stage and load cell were in a fast feedback loop, which kept stress constant to a minimum of ±0.5% the required value at all times.

All measurements were performed by mounting fresh strips of the non-aligned (polydomain) sample into the chamber and subsequently bringing it to a set tension by the motorized stage, followed by a heating ramp of the chamber at a constant rate while recording the sample temperature and the length. The incompressibility of the polymeric material was assumed, which allowed the direct calculation of stress (engineering and true) at each stage of deformation from the recorded shape of the deformed sample strip.

3. Model transient network: SIS

In this section, we discuss the creep measurements on the reference SIS elastomer. Well below T_g(PS) the material behaves as a classical rubber, and we measure the expected linear stress-strain

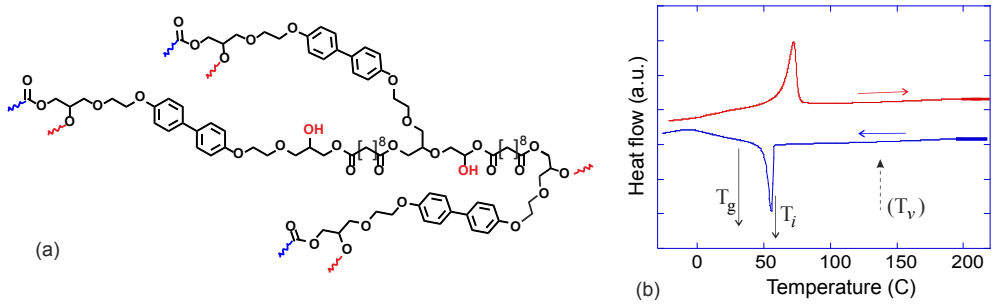

Fig. 3. (a) The chemical structure of xLCE2 chains, similar to xLCE but with slightly longer spacers between mesogenic groups. (b) The DSC scan of xLCE2 showing the (much lower) glass and smectic-isotropic transitions, T_g and T_i, respectively. The point T_v is also marked from our creep-experiment analysis.

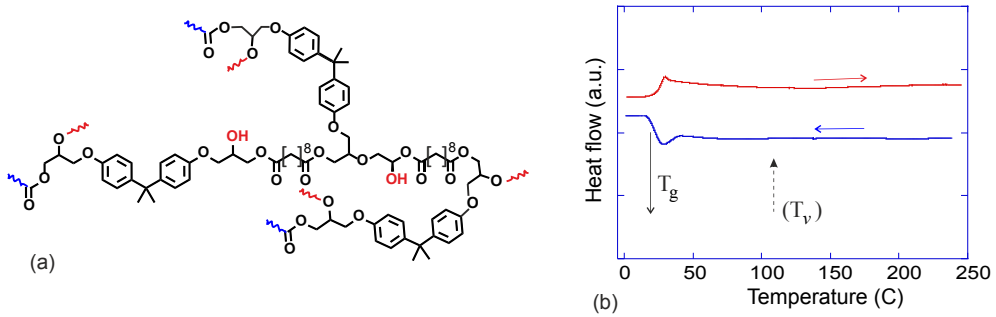

Fig. 4. (a) The chemical structure of classical vitrimer [5]. (b) The corresponding DSC scan showing the glass transitions T_g. The point T_v is also marked from our creep-experiment analysis.

relation $\sigma = E\varepsilon$ with the Young modulus $E \approx 923$ kPa at 22 °C and a low strain rate of ~$8 \cdot 10^{-4}$ s^{-1}. However, one must be careful with the issue of equilibrium even in a classical rubber: the stress relaxation is a very long process and no experiment can reach the true equilibrium (in all cases one has to make a decision: which level of relaxation is deemed sufficient for the current purpose). Fig. 5(a) illustrates this point: as in all rubbers, it is difficult to distinguish between the logarithmic or low-exponent power-law relaxation at very long times after the initial application of constant tension. After the initial fast relaxation taking seconds to minutes, the elastomer loses an additional 20% of the modulus (or increases its creep compliance $J = 1/E$ by 20%) in a day of further relaxation. There is much discussion of this long-time stress relaxation in rubbers in the old literature, but ultimately no analytical theory that describes it accurately [21]. In subsequent experiments, we regarded a full-day relaxation at a constant low temperature as sufficient for the heating transition experiments, because these heating experiments test the material on the time scale of minutes to hours and the remaining rubber relaxation is insignificant on these relatively short time scales.

Fig. 5(b) shows an example of our main experiment on thermal creep. After the sufficient relaxation ($t_{ref} = 1$ day), remaining at the constant tensile stress, the elastomer is heated at a constant rate of ~5°/min. The curve for tensile load of 400 kPa is the continuation of the preceding relaxation curve in plot (a). The fact that stress (or creep compliance) relaxation is not strictly completed is irrelevant now because the whole heating ramp takes less than 20 min, and on this time scale no residual relaxation is apparent. Initially we

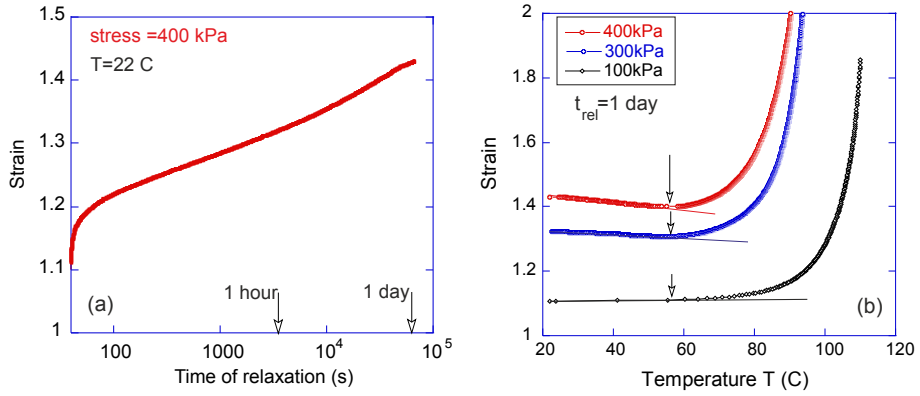

Fig. 5. (a) The 'creep compliance' relaxation for SIS at constant tensile stress and temperature, showing the remaining portion of short-time relaxation and the long relaxation over a period of a full day. The logarithmic scale of time emphasizes the lack of true equilibrium in the strain-stress relation $\varepsilon(t) = J(t)\sigma$. (b) The 'dilatometry' curves for SIS. At temperatures below T_v we see the classical effect of entropic elasticity, demonstrated by the linear dependence of rubber modulus on T (valid at constant cross-linking density). The point where the data deviates from this linear relation is identified as the transition to plastic flow, the vitrification point T_v: apparently it does not depend on the applied stress.

find the classical effect of entropic elasticity prominent: the linear stress-strain relation has its modulus (*e.g.,* the Young modulus, $E = 1/J$) linearly increasing with temperature, which causes the sample contraction highlighted by a straight line fitted to the relevant portion of the data. The slope of this decrease, $\varepsilon(T) = J(T)\sigma$, is a measure of the constant cross-linking density in the network. When at a certain characteristic temperature the data deviates from this extrapolated straight line, this reflects the loss of elastically active cross-links when the effective modulus decreases and (still at constant stress) the sample elongates increasingly, *i.e.,* the transition to the plastic-flow regime occurs.

This discussion and analysis help us identify the temperature of this 'vitrification' transition T_v, a method that we consistently used in the rest of this paper to identify T_v of different vitrimers. We suggest that this is the correct method based on the change of physical response of the stretched network – as opposed to looking at the point of strain divergence and the elastomer strip breaking down, which is strongly affected by the rate of heating and the internal relaxation dynamics in the network.

Note that this temperature of plastic transition does not have a strong dependence on the applied stress – and it is well below the bulk glass transition of polystyrene, $T_g \approx 100$ °C, or even the T_g(PS) ≈ 75 °C detected in this block-copolymer by calorimetry, see Fig. 1(b). This is because the release of each chain from a glassy PS micelle is an activation process of overcoming an energy barrier. The rate of chain release will be proportional to $\exp[-(\Delta G(T) - f\Delta x)/k_B T]$, where $\Delta G(T)$ is the temperature-dependent energy barrier to overcome for the pullout of the chain end, and $f\Delta x$ is the work done by the force applied the chain. In the case of SIS, it is clear that ΔG must be much larger than $f\Delta x$ until the temperature is close to T_g (at zero stress), as there is no obvious change in the observed T_v with stress (or force). The effect of imposed stress is also hidden by the relative high heating rate, where too few chains will have the chance to escape in the short period of time just below T_v where ΔG will be comparable to $f\Delta x$. To observe any lowering of T_v with imposed stress, a much lower heating rate is required; however, this comes with the additional problem of viscoelastic creep, with longer experimental times contributing to strain relaxation.

4. Smectic liquid crystal vitrimer: xLCE

The smectic liquid crystal phase of xLCE has a strong effect on the mechanical properties of the network. Smectic layers impose a strong constraint on the movement of network cross-links, which can slide in the layer plane but need to overcome a significant barrier to cross the layers [12,13]. In a polydomain smectic state, as we are working with, this constraint results in at least an order of magnitude increase in the effective Young modulus, see Fig. 6. On further increasing the strain, the material enters the stress-alignment regime (also called the polydomain-monodomain transition in LCEs [22,23]) during which different smectic domains randomly rotate and layers reorganise, releasing local stress. This leads to the dramatic softening of the elastomer during this regime of stress-alignment of smectic texture. However, after the release of imposed deformation the network retains most of its acquired shape (the shape-memory effect seen in Fig. 6 and discussed in much detail in Refs. [11,14]) because the new configuration of smectic layers restrains the cross-links, in their new positions. This is demonstrated in the hysteresis curve at 80 °C, where linear stress strain parts at the onset of stress and release of stress cover roughly the same strain (~10%), beyond this strain the elastomer can no longer elongate without the reordering of smectic layers. This new shape is "retained" until the material is heated into the isotropic phase, when the smectic order and the local orientational anisotropy melt and the network adopts its equilibrium stress-free shape determined by the cross-link configuration. Cooling back down to the smectic LC phase will re-establish the polydomain texture with no macroscopic shape change, *i.e.,* erase the memory of shape acquired during the deformation.

However, when the polymer network is capable of transesterification, there is no unique equilibrium shape of the network. At temperatures above the point of vitrification T_v, (irreversible) plastic flow will occur under external stress. Transesterification is an activation reaction, so in principle it occurs at lower temperatures too but with very low rates – making its effect insignificant below T_v. We now turn to the analysis of vitrification (the transition between elastic and plastic deformation regimes) in xLCE. Fig. 7 shows the results of our main experiment in the standard rheological "creep compliance" geometry. A constant stress is applied to the strip of elastomer and its relative extension (strain $\varepsilon = \Delta L/L$) recorded. We follow the protocol established in the study of SIS (Fig. 5) by allowing a sufficiently long time for initial relaxation and then increasing the temperature at such a rate that the residual relaxation remains insignificant on the time scale of experiment.

There are two quite dramatic features in Fig. 7: the softening of the xLCE as it approaches the smectic-isotropic transition temperature, T_i, and the irreversible plastic flow at temperatures above T_v. The first effect is the stress-alignment of the smectic texture which causes the natural length of the network to increase along the externally imposed axis of anisotropy. Note that the material is able to withstand quite a significant tensile stress, but will break quickly at high stress once in the isotropic phase (this is a very reproducible feature in many repeated experiments). We have seen the same effect in Fig. 6, which shows stress up to 2 MPa with no breaking in the smectic phase, in contrast to the sample breaking below 500 kPa in the isotropic phase.

Once the isotropic transition temperature is reached, the spontaneous chain anisotropy (the LC orientational order) disappears and the elastomer network contracts back. This is the classical effect of thermal actuation in LCE [12,24,25], when the natural shape of the elastomer network follows the spontaneous degree of chain anisotropy. It is interesting to see that the isotropic transition temperature does not change with the applied uniaxial stress.

Once in the isotropic phase, the network behaves as a classical elastomer and one can detect the shallow entropic contraction on heating (more pronounced at higher imposed stress). As in Fig. 5(b), we define the vitrification temperature T_v as the point of deviation from this entropic elasticity effect, when the plastic flow regime sets in. We find that this temperature also remains approximately constant on increasing imposed stress, $T_v \approx 160$ °C for this xLCE material.

A comparison between xLCE samples with and without catalyst can be seen in Fig. 8. There is a shift of the smectic-isotropic transition temperature T_i, which is the consequence of having the 5 mol % of the non-mesogenic impurity (TED catalyst) in the network in one case. Such a shift of phase-ordering temperature with annealed impurities is well known in liquid crystal science [26,27]. Apart from that, the response has the same characteristic features: the stress alignment and sample elongation on approaching the isotropic phase, when the strength of the cross-link trapping in the layers reduces – and the dramatic length reduction above T_i when the polymer chains lose their orientational order. The main difference occurs around the vitrification temperature: it is apparent that the samples without catalyst do not have the vitrification transition, but remain an isotropic rubbery network above the smectic-isotropic transition. This shows that transesterification reaction, promoted by the catalyst, is responsible for the onset of network creep above T_v.

The 'dilatometry' curves of xLCE2 are shown in Fig. 9 with notable differences when compared to the original xlCE (in Fig. 7).

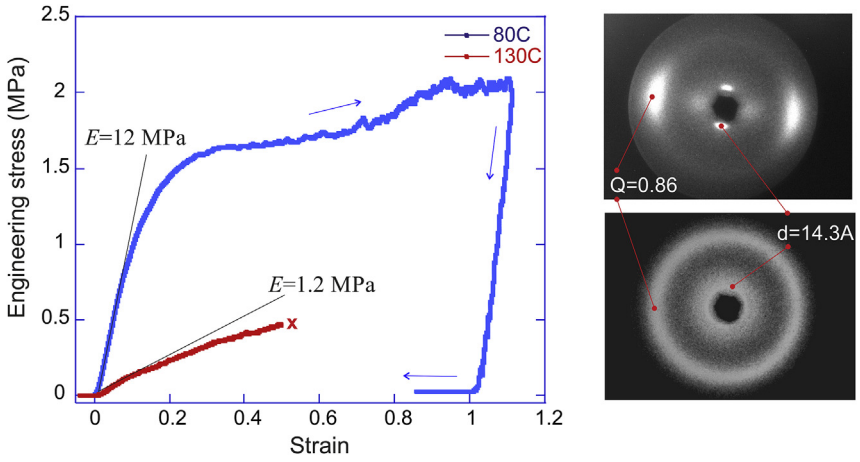

Fig. 6. The near-equilibrium stress-strain response of xLCE in the smectic phase (80 °C) and in the isotropic phase (130 °C) for comparison. The markedly different linear Young modulus is labeled on the plot. The X-ray images correspond to the points at the beginning of deformation when the smectic LC structure is polydomain, and the end of deformation when the smectic LC is well aligned in the direction of extension, showing a clear monodomain smectic-A diffraction pattern (the layer spacing d and the orientational nematic order parameter Q are labeled on the plot. The stress-alignment plateau of the polydomain-monodomain transition, and the shape-memory effect of the alignment retention are characteristic features of smectic LC elastomers [14,23].

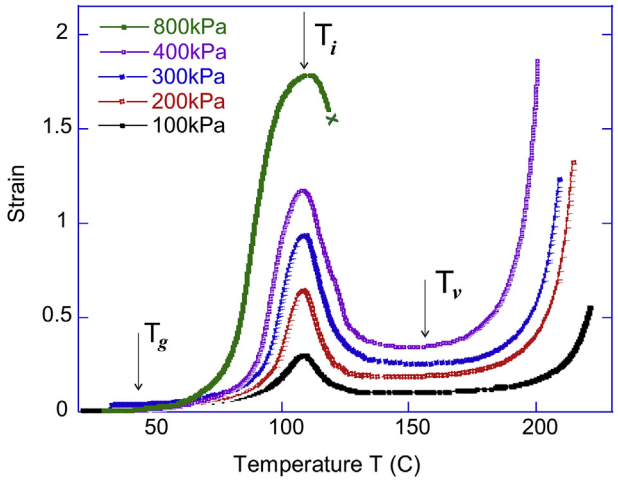

Fig. 7. The 'dilatometry' curves for xLCE showing the sequence of thermo-mechanical transitions in the smectic LCE vitrimer (in the presence of catalyst, *i.e.,* allowing for transesterification to proceed). The constant tensile stress applied is labeled on the plot. The network is very rigid even above its glass transition (in the smectic liquid-crystalline state), and only starts extension on the approach to the isotropic phase (at $T \rightarrow T_i$). The characteristic length contraction at $T > T_i$ is the classical 'thermal actuation' effect of stress-aligned elastomer contracts on losing its orientational order. Finally, at the vitrification temperature the samples start to plastically flow. Importantly, we find that neither T_i nor T_v change with increasing stress.

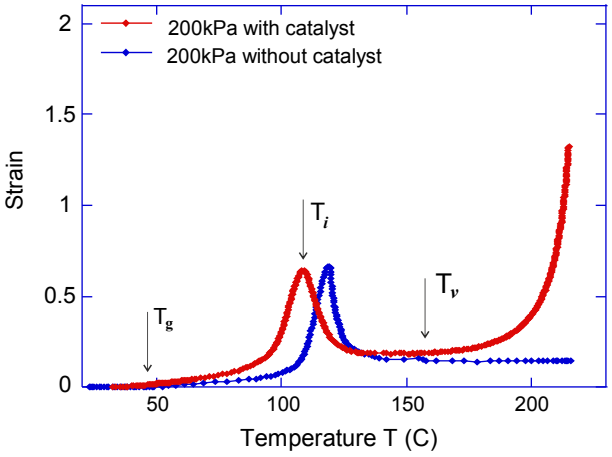

Fig. 8. The role of the TED catalyst in xLCE network: with transesterification process suppressed without the catalyst, the network remains an elastic rubber up to very high temperatures, while in the presence of catalyst it starts the plastic-flow regime above T_v.

The material is much more fragile at high temperatures, mainly because the smectic phase providing a significant mechanical strength in xLCE is now suppressed. In many experiments, we could not find the network surviving the tensile stress above 200 kPa. The most notable difference is absence of a strong thermal actuation effect above T_i, due to the glass transition and the smectic-isotropic transition clearly interfering with each other in this elastomer. However, typical LCE contraction is observed when heating a stress aligned xLCE as expected (not shown). As with xLCE, T_v is apparently independent of temperature.

Fig. 10 shows the 'dilatometry' curves for the classical vitrimer of Leibler et al. As with xLCE2 it was not possible to find any samples that survived above 200 kPa. This material has no liquid crystalline phase so only shows T_g and T_v effects. As before, there is no noticeable change in T_v with stress, and the observed vitrification temperature (~100 °C) was slightly lower than in the main xLCE. We note that T_v determined according to our procedure is significantly lower than reported by Leibler et al., [5,9] which is a result of its different definition.

5. Conclusions

We have examined the transition of an elastic polymer network into a plastic-flow regime, in the case when heating changes the nature of cross-links holding the network together. Our main interest was to investigate the vitrification point, *i.e.,* the temperature at or around which the physical reaction of a transient network to an applied stress changes from the entropic-elasticity response to the regime of plastic flow. It is easy and tempting to associate this plastic-flow regime with the point of divergence on the dilatometry curve – yet we demonstrate that the transition occurs earlier (while the point of divergence is a function of external factors such as heating rate). This identification is the main point of our paper.

On the dilatometry curves for SIS in Fig. 5(b), one might choose

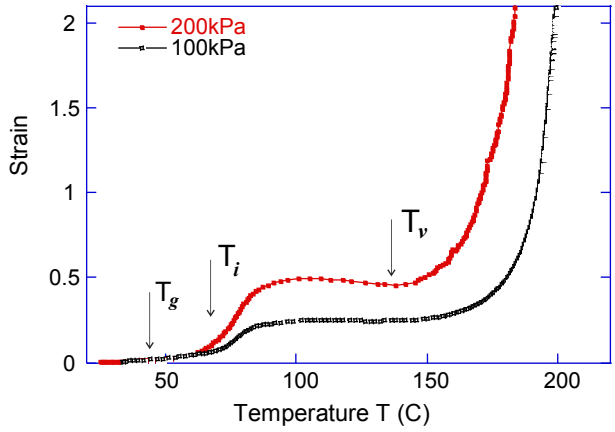

Fig. 9. The 'dilatometry' curves for xLCE2. The material is much more fragile at high temperatures, mainly because the smectic phase providing a significant mechanical strength in xLCE is now suppressed. In many experiments, we could not find the network surviving the tensile stress above 200 kPa. In fact, not allowing for a strong thermal actuation effect above T_i. The vitrification temperature (again, independent of stress applied) was slightly lower than in the main xLCE.

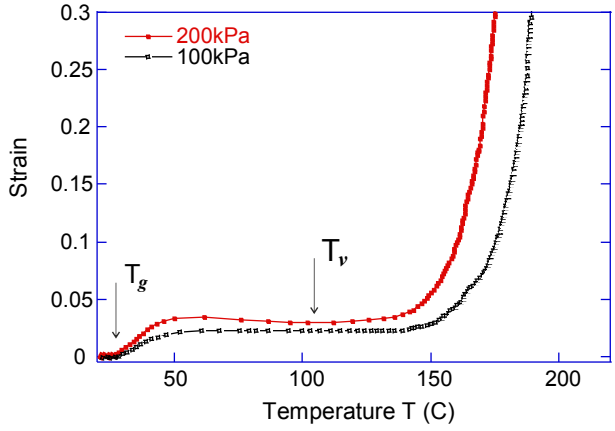

Fig. 10. The 'dilatometry' curves for the isotropic vitrimer of Leibler et al. The qualitative features of the constant-stress response are the same. with shallow entropic contraction in the elastomer region turning into the plastic creep at T_v, cf. Fig. 5(b).

different temperatures as the onset of plastic flow. However, the consistent assignment was made for the point of first deviation of the strain from its equilibrium rubber-elastic contraction with temperature. The key observation then was that T_v did not depend on the applied tension in any of the different materials studies. This was not a surprise in vitrimers, where the cross-link release is the catalytic transesterification reaction. However, in the physically bonded SIS this was a surprise. Our conclusion was that the onset of plastic flow occurs when the rate of cross-link release is still quite low (and the thermal-activation barrier high), so the effect of local tension was not noticeable.

The difference in thermal creep between the two xLCE materials was one of our points of interest. The close proximity of T_g and T_i in xLCE2 made the release of local mechanical constraints very slow and did not allow for any significant stress-alignment effects. There is little difference in thermo-mechanical behavior of xLCE2 and the isotropic vitrimer, even though the calorimetry and X-ray clearly show a prominent smectic phase in one of them. This was in contrast with xLCE with widely separated T_g and T_i, where effects of smectic stress-alignment and shape memory were prominent.

The other aspect of this work was to see the effects of smectic-A ordering and the associated shape-memory constraints in the transient network. In full agreement with many studies of permanently cross-linked smectic elastomers, greater applied stress causes dramatically greater lengthening as the temperature approaches T_i and the smectic layers align to stress. There is a correspondingly dramatic shortening of the elastomer as the temperature goes beyond T_i and the smectic ordering breaks down. If the liquid crystalline order was a permanent monodomain, this would be called thermal actuation – but in this case we are dealing with increasing stress-alignment and the retraction of order. Interestingly, we find the imposed stress does not alter the value of T_i itself. This observation needs to be considered in context of a naturally polydomain smectic texture in our materials. Misaligned smectic domains are regions of locally parallel layers of about 1 μm size separated by domain walls. The isotropic transition occurs due to interactions on the scale well below a single domain, while the mechanical response to stress is generated by the effects of elastic (in)compatibility between domains.

We hope the results of this work will guide the analysis and applications of transient networks, especially functional systems where the manipulation of internal liquid crystalline order leads to mechanical actuation.

Acknowledgments

This work was funded by the EPSRC (EP/J017639), the Ernest Oppenheimer Trust in Cambridge, and by China Scholarship Council. We are grateful to Jean Marshall for help with experimental techniques, and to Fanlong Meng for theoretical discussions.

References

[1] M. Yamamoto, J. Phys. Soc. Jpn. 11 (1956) 433.
[2] A.S. Lodge, Trans. Faraday Soc. 52 (1956) 120.
[3] F. Clement, A. Johner, J.-F. Joanny, A.N. Semenov, Macromolecules 33 (2000) 6148.
[4] A. Hotta, S.M. Clarke, E.M. Terentjev, Macromolecules 35 (2002) 271–277.
[5] D. Montarnal, M. Capelot, F. Tournilhac, L. Leibler, Science 334 (2011) 965–968.
[6] J.P. Brutman, P.A. Delgado, M.A. Hillmyer, ACS Macro Lett. 3 (2014) 607–610.
[7] W.D.G. Rivero, R. Nicolaÿ, L. Leibler, J.M. Winne, F.E.D. Prez, Adv. Funct. Mater. 5 (2015) 2451–2457.
[8] Y.-X. Lu, F. Tournilhac, L. Leibler, Z. Guan, J. Am. Chem. Soc. 134 (2012) 8424–8427.
[9] M. Capelot, M.M. Unterlass, F. Tournilhac, L. Leibler, ACS Macro Lett. 1 (2012) 789–792.
[10] M. Warner, E.M. Terentjev, Liquid Crystal Elastomers, Oxford University Press, Oxford, 2003.
[11] Z. Pei, Y. Yang, Q. Chen, E.M. Terentjev, Y. Wei, Y. Ji, Nat. Mater. 13 (2014) 36–41.
[12] E. Nishikawa, H. Finkelmann, Macromol. Chem. Phys. 200 (1999) 312–322.
[13] M.J. Osborne, E.M. Terentjev, Phys. Rev. E 62 (2000) 5101–5114.
[14] I.A. Rousseau, P.T. Mather, J. Am. Chem. Soc. 125 (2003) 15300–15301.
[15] I. Bellin, S. Kelch, R. Langer, A. Lendlein, Proc. Nat. Acad. Sci. U. S. A. 103 (2006) 18043–18047.
[16] T. Xie, Nature 464 (2010) 267–270.
[17] J.M. Widmaier, G.C. Meyer, Macromolecules 14 (1981) 450–452.
[18] T.G. Fox, P.J. Flory, J. Polym. Sci. 14 (1954) 315–319.
[19] S.A. Baeurle, A. Hotta, A.A. Gusev, Polymer 46 (2005) 4344–4354.
[20] B. Morèse-Séguéla, M. St-Jacques, J.M. Renaud, J. Prud'homme, Macromolecules 13 (1980) 100–106.
[21] A.D. Roberts, Natural Rubber Science and Technology, Clarendon Press, Oxford, England, 1988.
[22] S.V. Fridrikh, E.M. Terentjev, Phys. Rev. E 60 (1999) 1847–1857.
[23] C. Ortiz, M. Wagner, N. Bhargava, C.K. Ober, E.J. Kramer, Macromolecules 31 (1998) 8531–8539.
[24] J. Küpfer, H. Finkelmann, Macromol. Rapid Commun. 12 (1991) 717–721.
[25] A.R. Tajbakhsh, E.M. Terentjev, Eur. Phys. J. E 6 (2001) 181–188.
[26] P. Mukherjee, Liq. Cryst. 22 (1997) 239–243.
[27] V.J. Anderson, E.M. Terentjev, S.P. Meeker, J. Crain, W.C.K. Poon, Eur. Phys. J. E 4 (2001) 11–20.